

VIBRATION SUPPRESSION IN A FLEXIBLE GYROSCOPIC SYSTEM USING MODAL COUPLING STRATEGIES

SULTAN A. Q. SIDDIQUI and M. FARID GOLNARAGHI

*Construct Group, Department of Mechanical Engineering, University of Waterloo,
Waterloo, Ontario N2L 3G1, Canada*

Accepted for publication by Dr. Gary Anderson

(Received February 28, 1995)

Several recent studies have shown that vibrations in a two-degree-of-freedom system can be suppressed by using modal coupling based control techniques. This involves making the first two natural frequencies commensurable (e.g., in a ratio of 1:1 or 1:2) to establish a state of Internal Resonance (IR). When the system exhibits IR, vibrations in the two directions are strongly coupled resulting in a beat phenomenon. Upon introducing damping in one direction, oscillations in both directions can be quickly suppressed. In this paper we consider vibration suppression of a flexible two-degree-of-freedom gyroscopic system using 1:1 and 1:2 IR. The possibility of using 1:1 and 1:2 IR to enhance the coupling in the system is established analytically using the perturbation method of multiple scales. The results of IR based control strategy are compared with a new method, which is based on tuning the system parameters to make the mode shapes identical. Results indicate that this new technique is more efficient and easy to implement than IR based control strategies. Another advantage of this method is that there is no restriction on the frequencies as in the case of IR. Finally, a control torque is obtained which on application automatically tunes the system parameters to establish modal coupling.

KEYWORDS: *Vibration suppression; modal coupling; internal resonance*

1. INTRODUCTION

In this paper, we address vibration suppression of a flexible two-degree-of-freedom gyroscopic system with an uncontrollable mode. Using conventional control techniques it is generally not possible to regulate vibrations in such cases using one actuator because one mode is uncontrollable. However if the oscillations are coupled, the coupling may be utilized to regulate the oscillations indirectly. The vibration suppression strategy presented in this work is based on using a simple control scheme like a PD controller to regulate the vibrations in one direction and using the coupling to control the vibrations in the other direction. To effectively employ this strategy, the coupling has to be enhanced. Several recent studies [1–11] have suggested the use of the phenomenon of Internal Resonance (IR) as a means to enhance the coupling effect.

A system is said to be in a state of IR if the natural frequencies (Ω) are commensurable (i.e., $a_1 \Omega_1 + a_2 \Omega_2 + \dots = 0$, where a 's are positive or negative integers). When IR is established, the existing coupling between the two coordinate directions is enhanced. At this state, energy is continually exchanged between the modes resulting in a beat

phenomenon. Control is achieved upon introducing damping into one of the directions, from where the energy is dissipated leading to vibration suppression in both directions.

One of the first authors to investigate IR was Sethna [12]. Later several authors, Stupnicka [13], Van Dooren [14], Haddow *et al.* [15], and Mook *et al.* [16] studied resonant response of a system under harmonic excitation forces. Nayfeh and Mook [17] in their book give a comprehensive treatment on this subject. These studies reveal that the choice of IR ratio depends on the type of coupling in the system. When quadratic coupling is present, 1:2 IR ratio gives amplitude modulated response, and for cubic nonlinearities both 1:1 and 1:3 IR ratios can be used [17].

The research in Construct group at University of Waterloo has focused on applications of linear and nonlinear coupling terms to suppress vibrations. The first study in this area is the work by Golnaraghi [1,2], where he used a sliding mass to control the vibrations of a flexible cantilever beam. The controller in this work introduced an additional degree of freedom and kinematic nonlinearities to the system. In this case, control was achieved when the sliding mass motion was slightly damped at the state of 2:1 IR. Subsequently, Tuer *et al.* [3] and Duquette *et al.* [4] experimentally studied a flexible cantilever beam. The coupling in their system was introduced through a rigid beam that was attached to the tip of the flexible beam via a DC motor. Tuer [5] and Duquette [6] also discussed the use of linear coupling in vibration suppression of a cantilever beam. In more recent studies, enroute to generalize these control schemes, Tuer *et al.* [7,8] utilized coordinate coupling (linear coupling through position coordinates) and IR with quadratic coupling methods in active configurations. In these studies, the secondary degree of freedom was introduced in computer software and the coupling effect was introduced via an actuator connected to the plant. The example used by Tuer [7,8] was a flexible arm manipulator, and was tested experimentally for the case of coordinate coupling. The IR case was later tested by Oueini and Golnaraghi [9], experimentally. Later on, Khajepour *et al.* [10,11] used the center manifold and normal form methods to address the deficiencies of earlier studies and derived design criteria for the generalized coupling control law using quadratic nonlinearities.

In the above mentioned references, 1:2 IR ratio was predominantly used because quadratic nonlinearities were introduced in the system through the controller. However, in gyroscopic systems, the required coupling between the two degrees of freedom exists naturally, due to the gyroscopic forces. This makes gyroscopic type systems a natural candidate for the application of modal coupling based control strategies.

Gyroscopic systems in general can exhibit both linear and nonlinear couplings. For the system under consideration the equations of motion are coupled through linear, quadratic, and cubic terms. Therefore, we can investigate modal coupling through 1:1 and 1:2 frequency ratios. The existence of modal coupling for 1:1 and 1:2 IR is established analytically using the perturbation method of multiple scales and the results are verified numerically. In addition we also present a new vibration suppression strategy which uses the linear velocity coupling that arises through the gyroscopic terms and tunes the linear mode shapes directly to strengthen the link between the two degrees of freedom. It can be shown that 1:1 IR ratio forms a special case of this method. Numerical simulations show that, for gyroscopic systems, this method is more effective in suppressing vibrations than the method of IR. Investigations in the parameter space show that the system cannot be always tuned to exhibit a desired modal coupling. To overcome this, we present a control

law, which will make the system exhibit modal coupling, regardless of the values of the system parameters. This approach opens a new horizon for vibration suppression in other types of systems, on which we will be focusing in the early future.

2. SYSTEM DESCRIPTION AND MATHEMATICAL MODELING

The system studied is shown in Figure 1. A discrete model of a flexible beam of mass m and length l is assumed. The flexibility is modeled as two linear rotational springs of stiffness k_1 and k_2 in the vertical and horizontal planes, respectively. The beam is assumed to rotate at a constant angular velocity ω about the vertical axis. The rotation of the beam contributes to the centrifugal and gyroscopic forces on the system. The motion is described by the angular coordinates θ_1 and θ_2 . Further, the θ_1 direction is assumed as the control direction to which the controller is applied and the oscillations in the θ_2 direction are controlled indirectly through the coupling. The model retains many fundamental characteristics of physical gyroscopic systems like helicopter rotors, but at the same time it is simple enough to conduct analytical investigations. A detailed study of the gyroscopic characteristics of helicopter rotor blades can be found in [18,19].

Using the Lagrangian method the following equations of motion are obtained [20]:

$$\begin{aligned}
 & \begin{bmatrix} 1 & 0 \\ 0 & \cos^2(\theta_1) \end{bmatrix} \begin{bmatrix} \ddot{\theta}_1^* \\ \ddot{\theta}_2^* \end{bmatrix} + \begin{bmatrix} 0 & \frac{1}{2}\dot{\theta}_2^* \sin(2\theta_1) \\ -\dot{\theta}_2^* \sin(2\theta_1) & 0 \end{bmatrix} \begin{bmatrix} \dot{\theta}_1^* \\ \dot{\theta}_2^* \end{bmatrix} \\
 & + \begin{bmatrix} 0 & \omega^* \sin(2\theta_1) \\ -\omega^* \sin(2\theta_1) & 0 \end{bmatrix} \begin{bmatrix} \dot{\theta}_1^* \\ \dot{\theta}_2^* \end{bmatrix} + \begin{bmatrix} \omega_1^{*2} & 0 \\ 0 & \omega_2^{*2} \end{bmatrix} \begin{bmatrix} \theta_1 \\ \theta_2 \end{bmatrix} \\
 & + \begin{bmatrix} \frac{1}{2}\omega^{*2} \sin(2\theta_1) - \cos(\theta_1) + T^* & \\ & 0 \end{bmatrix} = \begin{bmatrix} 0 \\ 0 \end{bmatrix} \tag{1}
 \end{aligned}$$

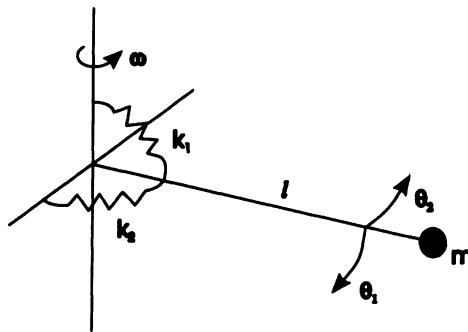


Figure 1 System model.

Similar equations are obtained in [18] in connection with a rigid body model of a helicopter rotor blade. In (1), nondimensional parameters are used which are defined as follows:

$$t^* = \sqrt{\frac{g}{l}} t, \frac{d}{dt^*} = \sqrt{\frac{l}{g}} \frac{d}{dt}, \frac{d^2}{dt^{*2}} = \frac{l}{g} \frac{d^2}{dt^2}$$

$$\omega^* = \sqrt{\frac{l}{g}} \omega, \omega_1^{*2} = \frac{k_1}{mgl}, \omega_2^{*2} = \frac{k_2}{mgl} \quad (2)$$

and θ_1^* , θ_2^* , $\dot{\theta}_1^*$, and $\dot{\theta}_2^*$ denote the nondimensionalized rates. In (1) the term T^* represents the controller torque that is applied along θ_1 . To illustrate the modal coupling strategies, we assume Proportional and Derivative (PD) feedback control. Using PD control, T^* is defined as follows:

$$T^* = K(\theta_{1r} - \theta_1) + C\dot{\theta}_1^* \quad (3)$$

where K is the controller position gain, C is the controller velocity gain and θ_{1r} is a constant reference input. Another term T_c^* , which represents the constant element in (3) is defined as follows:

$$T_c^* = K\theta_{1r} \quad (4)$$

Using (3) and (4), the equations of motion (1) are written as follows:

$$\begin{aligned} & \begin{bmatrix} 1 & 0 \\ 0 & \cos^2(\theta_1) \end{bmatrix} \begin{bmatrix} \dot{\theta}_1^* \\ \dot{\theta}_2^* \end{bmatrix} + \begin{bmatrix} 0 & \frac{1}{2}\dot{\theta}_2^* \sin(2\theta_1) \\ -\dot{\theta}_2^* \sin(2\theta_1) & 0 \end{bmatrix} \begin{bmatrix} \theta_1^* \\ \theta_2^* \end{bmatrix} \\ & + \begin{bmatrix} C & \omega^* \sin(2\theta_1) \\ -\omega^* \sin(2\theta_1) & 0 \end{bmatrix} \begin{bmatrix} \dot{\theta}_1^* \\ \dot{\theta}_2^* \end{bmatrix} + \begin{bmatrix} \omega_{n1}^{*2} & 0 \\ 0 & \omega_{n2}^{*2} \end{bmatrix} \begin{bmatrix} \theta_1 \\ \theta_2 \end{bmatrix} \\ & + \begin{bmatrix} \frac{1}{2}\omega^{*2} \sin(2\theta_1) - \cos(\theta_1) + T_c^* \\ 0 \end{bmatrix} = \begin{bmatrix} 0 \\ 0 \end{bmatrix} \end{aligned} \quad (5)$$

where ω_{n1}^* and ω_{n2}^* (for notational consistency) are defined as:

$$\omega_{n1}^{*2} = \omega_1^{*2} - K$$

$$\omega_{n2}^{*2} = \omega_2^{*2} \quad (6)$$

The controller is used to tune the system parameters to establish modal coupling and to introduce damping in the θ_1 direction. From (6) it can be seen that by adjusting the controller position gain K , the value of ω_{n1}^* can be tuned to establish modal coupling in the system.

3. EQUILIBRIUM POSITIONS

The constant solution for (5) is defined as an equilibrium position. The equilibrium positions are obtained by setting velocity and accelerations to zero in (5) ($\dot{\theta}_1^* = \dot{\theta}_2^* = \ddot{\theta}_1^* = \ddot{\theta}_2^* = 0$), resulting in the following equations:

$$\begin{aligned} \omega_{n1}^{*2}\theta_{1e} + \frac{1}{2}\omega^{*2}\sin(\theta_{1e}) - \cos(\theta_{1e}) + T_c^* &= 0 \\ \omega_{n2}^{*2}\theta_{2e} &= 0 \end{aligned} \tag{7}$$

where θ_{1e} and θ_{2e} are the equilibrium values. From (7) it can be seen that θ_{2e} is always zero, but the equilibrium values for θ_{1e} depend on the system parameters ω^* , ω_{n1}^* , and T_c^* . It can be seen that the first equation in (7) is nonlinear, so multiple equilibrium values could exist for θ_1 . When the system parameters are varied the equilibrium positions change, and by adjusting the controller reference input θ_{1r} , the value of T_c^* and, hence, the equilibrium position can be tuned to a desired value.

The stability of the equilibrium positions can be established using the eigenvalues of the linearized equations of motion or the Lyapunov's direct method. Figure 2 shows the equilibrium values for θ_1 and also points a stable equilibrium position. A detailed investigation of the stability of the equilibrium positions for this system was conducted in [20]. In this paper we consider motion only about the stable equilibria.

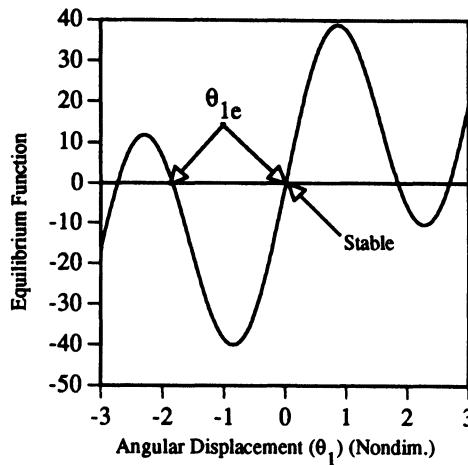


Figure 2 Equilibrium function; $\omega^* = 8.0$, $\omega_{n1}^* = 3.0$, $T_c^* = 0$.

4. MOTION IN THE NEIGHBORHOOD OF EQUILIBRIUM POINTS

To investigate the motion in the neighborhood of equilibrium points, the equations of motion (5) are expanded about the equilibrium position. In the analysis which follows, the controller velocity gain C is assumed to be small and neglected for simplicity. Using Taylor series expansion about an equilibrium point and collecting terms up to third order we obtain the following approximate equations of motion:

$$\begin{bmatrix} 1 & 0 \\ 0 & 1 \end{bmatrix} \begin{bmatrix} \ddot{u}_1 \\ \ddot{u}_2 \end{bmatrix} + \begin{bmatrix} 0 & s_1 \\ s_6 & 0 \end{bmatrix} \begin{bmatrix} \dot{u}_1 \\ \dot{u}_2 \end{bmatrix} + \begin{bmatrix} s_2 & 0 \\ 0 & s_7 \end{bmatrix} \begin{bmatrix} u_1 \\ u_2 \end{bmatrix} = \begin{bmatrix} s_3 s_1^2 + s_4 \dot{u}_2^2 + s_5 u_1 \dot{u}_2 + s_{11} u_1^3 + s_{12} u_1^2 \dot{u}_2 + s_{13} u_1 \dot{u}_2^2 \\ s_8 \dot{u}_1 \dot{u}_2 + s_9 u_1 \dot{u}_1 + s_{10} u_1 u_2 + s_{14} u_1 \dot{u}_1 \dot{u}_2 + s_{15} u_1^2 \dot{u}_1 + s_{16} u_1^2 u_2 \end{bmatrix} \quad (8)$$

where $u_1 = \theta_1 - \theta_{1e}$, and $u_2 = \theta_2 - \theta_{2e}$ and the s_1 terms are given by:

$$\begin{aligned} s_1 &= \omega^* \sin(2\theta_{1e}), & s_2 &= \omega^{*2} \cos(2\theta_{1e}) + \omega_{n1}^{*2} + \sin(\theta_{1e}) \\ s_3 &= -\frac{1}{2} \cos(\theta_{1e}) + \omega^{*2} \sin(2\theta_{1e}), & s_4 &= -\frac{1}{2} \sin(2\theta_{1e}) \\ s_5 &= -2\omega^* \cos(2\theta_{1e}), & s_6 &= -2\omega^* \tan(\theta_{1e}) \\ s_7 &= \omega_{n2}^{*2} \sec^2(\theta_{1e}), & s_8 &= \sin(2\theta_{1e}) \sec^2(\theta_{1e}) \\ s_9 &= 2\omega^* \sec^2(\theta_{1e}), & s_{10} &= -2\omega_{n2}^{*2} \tan(\theta_{1e}) \sec^2(\theta_{1e}) \\ s_{11} &= \frac{2}{3} \omega^{*2} \cos(2\theta_{1e}) + \frac{1}{6} \sin(\theta_{1e}), & s_{12} &= 2\omega^* \sin(2\theta_{1e}) \\ s_{13} &= -\cos(2\theta_{1e}), & s_{14} &= 2 \sec^2(\theta_{1e}) \\ s_{15} &= 2\omega^* \sin(\theta_{1e}) \sec^3(\theta_{1e}), & s_{16} &= \omega_{n2}^{*2} (2 \cos^2(\theta_{1e}) - 3) \sec^4(\theta_{1e}) \end{aligned} \quad (9)$$

The equations of motion (8) are used later in the perturbation analysis to establish modal coupling under resonant conditions.

5. CHARACTERISTIC ROOTS

Assuming $u_i = a_i e^{i\Omega t}$ as the solution of the linearized equations associated with (8), we obtain the following characteristic equation:

$$\Omega^4 - (s_2 + s_7 - s_1 s_6) \Omega^2 + s_2 s_7 = 0 \quad (10)$$

where the roots Ω_i are given by:

$$\begin{aligned}\Omega_{1,2}^2 &= \frac{(s_2 + s_7 - s_1 s_6) \pm \sqrt{(s_2 + s_7 - s_1 s_6)^2 - 4s_2 s_7}}{2} \\ &= \frac{(s_2 + s_7 - s_1 s_6) \pm \sqrt{(s_2 - s_7 - s_1 s_6)^2 - 4s_1 s_6 s_7}}{2}\end{aligned}\quad (11)$$

Note that

$$-4s_1 s_6 s_7 = 4\omega^{*2} \omega_{n2}^{*2} \tan^2(2\theta_{1e}) \geq 0 \quad (12)$$

therefore Ω_1^2 and Ω_2^2 , corresponding to the eigenvalues of the linear portion of (8) are always real, and the natural frequencies Ω_1 and Ω_2 are associated with the positive roots of Ω_1^2 and Ω_2^2 , respectively.

6. PERTURBATION EXPANSIONS

The perturbation analysis in the case of 1:1 or 1:2 IR is performed using the method of multiple scales. Details of this method can be found in [17] and [21]. Following the procedure of the multiple scales method the dependent variables u_1 and u_2 are assumed as follows:

$$\begin{aligned}u_1 &= \varepsilon u_{11}(T_0, T_1, T_2) + \varepsilon^2 u_{12}(T_0, T_1, T_2) + \varepsilon^3 u_{13}(T_0, T_1, T_2) \\ u_2 &= \varepsilon u_{21}(T_0, T_1, T_2) + \varepsilon^2 u_{22}(T_0, T_1, T_2) + \varepsilon^3 u_{23}(T_0, T_1, T_2)\end{aligned}\quad (13)$$

where ε represents a nondimensional scaling parameter, and u_{1i} and u_{2i} ($i = 1 \dots 3$) represent the solution corresponding to the order ε^i . Since we use three terms in the expansion for u_1 and u_2 , multiple scales method requires that the nondimensional time t^* is also measured on three different time scales T_0 , T_1 , and T_2 , which are defined as follows:

$$T_i = \varepsilon^i t^*; \quad i = 0, 1, \text{ and } 2 \quad (14)$$

The scale T_0 is a fast scale and T_1 , T_2 represent slower time scales. Using the chain rule of differentiation and (14), the derivatives with respect to the nondimensional time t^* are written as follows:

$$\begin{aligned}\frac{d}{dt^*} &= D_0 + \varepsilon D_1 + \varepsilon^2 D_2 \\ \frac{d}{dt^*} &= D_0^2 + 2\varepsilon D_0 D_1 + \varepsilon^2 (2D_0 D_2 + D_1^2)\end{aligned}\quad (15)$$

where D_i represents the partial derivatives with respect to T_i .

Substituting (13) and (15) in the equations of motion (8), and collecting like powers of ϵ , gives the following equations:

Order ϵ :

$$\begin{aligned} D_0^2 u_{11} + s_1 D_0 u_{21} + s_2 u_{11} &= 0 \\ D_0^2 u_{21} + s_6 D_0 u_{11} + s_7 u_{21} &= 0 \end{aligned} \quad (16)$$

Order ϵ^2 :

$$\begin{aligned} D_0^2 u_{12} + s_1 D_0 u_{22} + s_2 u_{12} &= -2D_0 D_1 u_{11} - s_1 D_1 u_{21} + s_3 u_{11}^2 + s_4 (D_0 u_{21})^2 \\ &\quad + s_5 u_{11} D_0 u_{21} \\ D_0^2 u_{22} + s_6 D_0 u_{12} + s_7 u_{22} &= -2D_0 D_1 u_{21} - s_6 D_1 u_{11} + s_8 D_0 u_{11} D_0 u_{21} + s_9 u_{11} D_0 u_{11} \\ &\quad + s_{10} u_{11} u_{21} \end{aligned} \quad (17)$$

Order ϵ^3 :

$$\begin{aligned} D_0^2 u_{13} + s_1 D_0 u_{23} + s_2 u_{13} &= -2D_0 D_1 u_{12} - 2D_0 D_2 u_{11} - D_1^2 u_{11} - s_1 (D_1 u_{22} + D_2 u_{21}) \\ &\quad + 2s_3 u_{11} u_{12} + 2s_4 (D_0 u_{21} D_1 u_{21} + D_0 u_{21} D_0 u_{22}) \\ &\quad + s_5 (u_{11} D_0 u_{22} + u_{12} D_0 u_{21} + u_{11} D_1 u_{21}) \\ &\quad + s_{11} u_{11}^3 + s_{12} D_0 u_{21} u_{11}^2 + s_{13} (D_0 u_{21})^2 u_{11} \\ D_0^2 u_{23} + s_6 D_0 u_{13} + s_7 u_{23} &= -2D_0 D_1 u_{22} - 2D_0 D_2 u_{21} - D_1^2 u_{21} - s_6 (D_1 u_{12} + D_2 u_{11}) \\ &\quad + s_8 (D_1 u_{11} D_0 u_{21} + D_0 u_{11} D_0 u_{22} + D_0 u_{11} D_1 u_{21} + D_0 u_{12} D_0 u_{21}) \\ &\quad + s_9 (u_{12} D_0 u_{11} + u_{11} D_0 u_{12} + u_{11} D_1 u_{11}) + s_{10} (u_{12} u_{21} + u_{11} u_{22}) \\ &\quad + s_{14} D_0 u_{11} D_0 u_{21} u_{11} + s_{15} D_0 u_{11} u_{11}^2 + s_{16} u_{11}^2 u_{21} \end{aligned} \quad (18)$$

The perturbation technique involves solving (16), (17), and (18) sequentially. The general solution for (16) can be considered as:

$$\begin{aligned} u_{11} &= A_1(T_1, T_2) e^{i\Omega_1 T_0} + A_2(T_1, T_2) e^{i\Omega_2 T_0} + cc \\ u_{21} &= r_1 A_1(T_1, T_2) e^{i\Omega_1 T_0} + r_2 A_2(T_1, T_2) e^{i\Omega_2 T_0} + cc \end{aligned} \quad (19)$$

where cc denotes complex conjugate of the preceding terms, and A_1 and A_2 are, in general, functions of the slower time scales T_1 and T_2 , indicating that amplitudes vary slowly with time. In (19), r_1 and r_2 are the modal amplitude ratios corresponding to the first and second natural frequencies, respectively, and are given by:

$$\begin{aligned}
 r_1 &= -\frac{s_2 - \Omega_1^2}{is_1\Omega_1} = -\frac{is_6\Omega_1}{s_7 - \Omega_1^2} \\
 r_2 &= -\frac{s_2 - \Omega_2^2}{is_1\Omega_2} = -\frac{is_6\Omega_2}{s_7 - \Omega_2^2}
 \end{aligned} \tag{20}$$

The equations developed in this section are used to show the existence of modal coupling in the 1:1 and 1:2 IR cases, next.

7. VIBRATION SUPPRESSION USING 1:1 IR

The first vibration suppression strategy discussed is 1:1 IR. It requires tuning the value of ω_{n1}^* to make $\Omega_1 = \Omega_2$. For a given set of parameters it may not be always possible to obtain a real value for the tuning parameter ω_{n1}^* to establish a desired ratio of Ω_1 and Ω_2 . Therefore we first consider the problem of tuning the system parameters to establish IR.

7.1 System Parameters

From (11) it follows that the difference between the frequencies Ω_1 and Ω_2 is given by:

$$\Omega_1 - \Omega_2 = \sqrt{s_2 + s_7 - s_1s_6 - 2\sqrt{s_2s_7}} \tag{21}$$

If the difference between the frequencies is set to zero, from (21) the following equation is obtained:

$$s_2 = \sqrt{s_7} \pm \sqrt{s_1s_6} \tag{22}$$

It can be seen from (9) that s_1s_6 is a negative quantity, and from (22) it follows that s_2 and hence ω_{n1}^* are complex quantities implying that we cannot have an exact ratio of Ω_1 and Ω_2 . Since the system cannot be tuned to establish an exact 1:1 ratio of the natural frequencies, we try to minimize the difference between the frequencies with respect to the tuning parameter ω_{n1}^* . After simplification it results in the following equations:

$$\begin{aligned}
 s_2 &= s_7 \\
 \omega_{n1}^{*2} &= -\omega^{*2}\cos(2\theta_{1e}) - \sin(\theta_{1e}) + \omega_{n2}^{*2}\sec^2(\theta_{1e})
 \end{aligned} \tag{23}$$

When the system parameters are tuned according to (23) the difference between the natural frequencies, given by (21) is reduced to the following equation:

$$\begin{aligned}
 \delta &= \Omega_1 - \Omega_2 = \sqrt{-s_1s_6} \\
 &= 2\omega^* \sin(\theta_{1e})
 \end{aligned} \tag{24}$$

where δ is called the detuning parameter. It can be seen from (24) that for small values of θ_{1e} , δ is small and the frequencies can be considered to be approximately equal. For convenience we refer to this approximate ratio as 1:1 IR. For larger values of θ_{1e} , the value of δ is large and the system cannot be considered as 1:1 resonant. Figure 3(a) shows a set of values of ω_{n1}^* required for tuning the system to 1:1 IR when ω^* is varied. Figure 3(b) shows the natural frequencies along the same path. From this figure it can be seen that the range of the tuning parameter ω_{n1}^* is limited. To overcome this we present a method to modify the control torque in Section (9.1).

7.2 Perturbation Analysis

The perturbation analysis involves extensive algebraic manipulation, which is carried out using the symbolic manipulation program MAPLE. In carrying out the perturbation analysis the approach presented in [21] is adopted. The solution (19) of the order ϵ equations is substituted into the order ϵ^2 equations (17), and after simplification gives the

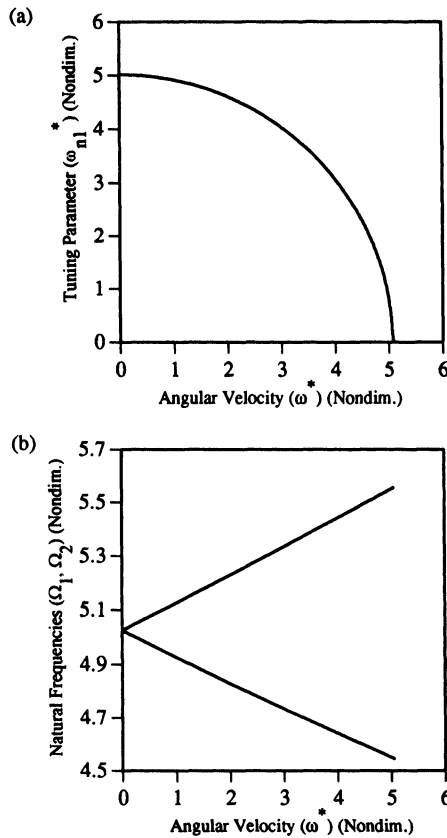


Figure 3 Tuned parameters and natural frequencies—1:1 IR $\omega_{n2}^* = 5.0$, $\theta_{1e} = 0.1$. (a) Tuned parameter values; (b) Natural frequencies along tuned path.

following expressions for the right-hand sides, denoted by *rhs3* and *rhs4*:

$$\begin{aligned}
 rhs3 &= x_1 A_1' e^{i\Omega_1 T_0} + x_2 A_2' e^{i\Omega_2 T_0} + x_3 A_1^2 e^{i2\Omega_1 T_0} + x_4 A_2^2 e^{i2\Omega_2 T_0} \\
 &\quad + x_5 A_1 A_2 e^{i(\Omega_1 + \Omega_2) T_0} + x_6 A_1 \bar{A}_2 e^{i(\Omega_1 - \Omega_2) T_0} + cc + x_7 A_1 \bar{A}_1 + x_8 A_2 \bar{A}_2 \\
 rhs4 &= x_9 A_1' e^{i\Omega_1 T_0} + x_{10} A_2' e^{i\Omega_2 T_0} + x_{11} A_1^2 e^{i2\Omega_1 T_0} + x_{12} A_2^2 e^{i2\Omega_2 T_0} \\
 &\quad + x_{13} A_1 A_2 e^{i(\Omega_1 + \Omega_2) T_0} + x_{14} A_1 \bar{A}_2 e^{i(\Omega_1 - \Omega_2) T_0} + cc
 \end{aligned} \tag{25}$$

where x_i , $i = 1 \dots 14$, are constants which depend on the system parameters and (') indicates differentiation with respect to T_1 . These constants are not presented because of the length of these terms. Since an exact 1:1 ratio of Ω_1 and Ω_2 cannot be established we use the detuning parameter δ . However we first scale δ by using $\delta = \epsilon^2 \sigma$ to give the correct time scale, and write (24) as follows:

$$\Omega_2 = \Omega_1 + \epsilon^2 \sigma \tag{26}$$

The terms $e^{\pm i\Omega_1 T_0}$ and $e^{\pm i\Omega_2 T_0}$ appear in both the homogeneous and the particular solution of (17), this gives rise to secular terms which makes the solution of (17) nonuniform. Eliminating the secular terms results in solvability conditions which relate the modal amplitudes A_1 and A_2 . To eliminate the secular terms from u_{12} and u_{22} , the following particular solution is assumed, which neglects all the terms except the ones which lead to secular terms:

$$\begin{aligned}
 u_{12} &= P_{11} e^{i\Omega_1 T_0} + P_{12} e^{i\Omega_2 T_0} \\
 u_{22} &= P_{21} e^{i\Omega_1 T_0} + P_{22} e^{i\Omega_2 T_0}
 \end{aligned} \tag{27}$$

Note in (27) that the conjugate terms are also neglected because they would lead to four incompatible equations relating A_1 and A_2 . Substituting (27) in (17) and equating the coefficients of $e^{i\Omega_1 T_0}$ and $e^{i\Omega_2 T_0}$ on both sides results in the following solvability conditions:

$$\begin{aligned}
 (k_2 - \Omega_n^2) P_{1n} + ik_1 \Omega_n P_{2n} &= R_{1n} \\
 ik_6 \Omega_n P_{1n} + (k_7 - \Omega_n^2) P_{2n} &= R_{2n}
 \end{aligned} \tag{28}$$

where $n = 1, 2$ and R_{1n} and R_{2n} are given by:

$$\begin{aligned}
 R_{11} &= x_1 A_1', R_{12} = x_2 A_2' \\
 R_{21} &= x_9 A_1', R_{22} = x_{10} A_2'
 \end{aligned} \tag{29}$$

For a nontrivial solution to (28) it requires that

$$\begin{vmatrix} s_2 - \Omega_n^2 & R_{1n} \\ is_6 \Omega_n & R_{2n} \end{vmatrix} = 0 \tag{30}$$

where s_2 and s_6 are defined in (9). Solving (30) for $n = 1, 2$ gives the following conditions:

$$A_1' = 0, A_2' = 0 \quad (31)$$

which imply that $A_1 = A_1(T_2)$, $A_2 = A_2(T_2)$ and the coupling between the modes cannot be established using ϵ^2 equations (17). Therefore, we have to consider the higher order equations (18). The first step involves substituting (31) in (25) and obtain the particular solution for (17) by considering the remaining terms in the right-hand sides. Substituting the homogeneous solution for u_{11} and u_{21} (19), and the particular solution for u_{21} and u_{22} in (18) results in the following terms for the right-hand sides of (18), denoted by *rhs5* and *rhs6*:

$$\begin{aligned} rhs5 &= \{x_{15}A_1'(T_2) + x_{16}A_1^2\bar{A}_1 + x_{17}A_1A_2\bar{A}_2\}e^{i\Omega_1T_0} \\ &+ \{x_{18}A_2'(T_2) + x_{19}A_1\bar{A}_1A_2 + x_{20}A_2^2\bar{A}_2\}e^{i\Omega_2T_0} \\ &+ x_{21}A_1^3e^{i3\Omega_1T_0} + x_{22}A_2^3e^{i3\Omega_2T_0} + x_{23}A_1A_2^2e^{i(2\Omega_2+\Omega_1)T_0} + x_{24}A_1^2A_2e^{i(2\Omega_1+\Omega_2)T_0} \\ &+ x_{25}A_1\bar{A}_2^2e^{i(\Omega_1-2\Omega_2)T_0} + x_{26}\bar{A}_1^2A_2e^{i(\Omega_2-2\Omega_1)T_0} + cc \\ rhs6 &= \{x_{27}A_1'(T_2) + x_{28}A_1^2\bar{A}_1 + x_{29}A_1A_2\bar{A}_2\}e^{i\Omega_1T_0} \\ &+ \{x_{30}A_2'(T_2) + x_{31}A_1\bar{A}_1A_2 + x_{32}A_2^2\bar{A}_2\}e^{i\Omega_2T_0} \\ &+ x_{33}A_1^3e^{i3\Omega_1T_0} + x_{34}A_2^3e^{i3\Omega_2T_0} + x_{35}A_1A_2^2e^{i(2\Omega_2+\Omega_1)T_0} + x_{36}A_1^2A_2e^{i(2\Omega_1+\Omega_2)T_0} \\ &+ x_{37}A_1\bar{A}_2^2e^{i(\Omega_1-2\Omega_2)T_0} + x_{38}\bar{A}_1^2A_2e^{i(\Omega_2-2\Omega_1)T_0} + cc \end{aligned} \quad (32)$$

where (') indicates differentiation with respect to T_2 , and x_i are constants. Using the resonant condition (26) the following relationships are obtained:

$$\begin{aligned} e^{i(-\Omega_2+2\Omega_1)T_0} &= e^{i\Omega_2T_0} e^{-i2\sigma T_2} \\ e^{-i(\Omega_1-2\Omega_2)T_0} &= e^{i\Omega_1T_0} e^{i2\sigma T_2} \end{aligned} \quad (33)$$

Substituting (33) in (32) and assuming a solution for u_{13} and u_{23} similar to (27), and equating the coefficients of similar terms on either side of (18), we obtain the following solvability conditions which establish the modal coupling:

$$\begin{aligned} x_{39}A_1'(T_2) + x_{40}A_1^2\bar{A}_1 + x_{41}A_1A_2\bar{A}_2 + x_{42}A_2^2\bar{A}_1e^{2i\sigma T_2} &= 0 \\ x_{43}A_2'(T_2) + x_{44}A_2^2\bar{A}_2 + x_{45}A_1A_2\bar{A}_1 + x_{46}A_1^2\bar{A}_2e^{-2i\sigma T_2} &= 0 \end{aligned} \quad (34)$$

The complex constants A_1 and A_2 are converted to polar form using:

$$\begin{aligned} A_1 &= \frac{1}{2} a_1 e^{i\alpha_1} \\ A_2 &= \frac{1}{2} a_2 e^{i\alpha_2} \end{aligned} \quad (35)$$

where $a_1(T_2)$ and $a_2(T_2)$ are modal amplitudes and $\alpha_1(T_2)$ and $\alpha_2(T_2)$ are phases of the response.

Using (35) the solvability conditions (34) are reduced to the following differential equations:

$$\begin{aligned} a_1' &= \Gamma_1 a_2^2 a_1 \sin(\gamma) \\ a_2' &= -\Gamma_2 a_1^2 a_2 \sin(\gamma) \\ \alpha_1' &= -2\Gamma_1 a_2^2 \cos(\gamma) + \Gamma_3 a_1^2 + \Gamma_4 a_2^2 \\ \alpha_2' &= -2\Gamma_2 a_1^2 \cos(\gamma) + \Gamma_5 a_1^2 + \Gamma_6 a_2^2 \end{aligned} \quad (36)$$

where

$$\gamma = 2\sigma T_2 - 2\alpha_1 + 2\alpha_2 \quad (37)$$

and Γ_i , $i = 1 \dots 6$ are constants which depend on system parameters and are too long to be included here, the reader is referred to [20] for their actual values. Using (37) the last two equations in (36) can be combined reducing the number of equations to three:

$$\gamma' = 2\sigma + 4(\Gamma_1 a_2^2 - \Gamma_2 a_1^2) \cos(\gamma) + 2(\Gamma_5 - \Gamma_3) a_1^2 + 2(\Gamma_6 - \Gamma_4) a_2^2 \quad (38)$$

Eliminating γ from the first two equations in (36) and integrating we get the following equation, which shows exchange of energy between the modes:

$$a_1^2 + \nu a_2^2 = E \quad (39)$$

In the above equation, $\nu = \Gamma_1/\Gamma_2$ and E is an integration constant which depends on the initial conditions and represents the modal energy. Equation (39) shows that the modal amplitudes are coupled and energy is exchanged between the modes. The system of equations (36) are solved numerically to illustrate the coupling between the modes. Figure 4 shows such a response for 1:1 IR tuned parameters. It illustrates that the amplitude modes a_1 and a_2 are strongly coupled and 1:1 IR can be successfully used to control the vibrations.

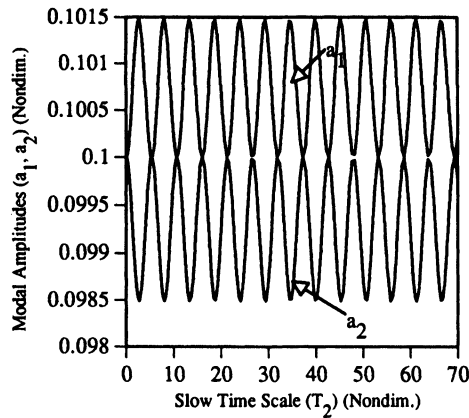


Figure 4 Modal amplitude response—1:1 IR. $\omega^* = 3.0$, $\omega_{n1}^* = 4.04$, $\omega_{n2}^* = 5.0$, $\theta_{1e} = 0.1$, $\sigma = -0.599$.

7.3 Numerical Simulations

To illustrate numerically the vibration suppression strategy, the nonlinear system of equations (5) are used. Figure 5 shows the time response for a set of 1:1 IR tuned parameters for the undamped case. The response shows distinctive beats which are typical for Internal Resonance. The response on the slow time scale T_2 , shown in Figure 4, represents the envelopes of the beats. When damping is introduced in the θ_1 direction using the controller velocity gain C , energy can be quickly dissipated from the system. This is illustrated in Figure 6 for different damping coefficients. These figures indicate that when C is increased we get an optimal response, Figure 6(b), and further increase in C does not improve the response because the oscillations in the θ_1 mode decay quickly and limit the interaction between the modes. To further analyze the role of damping, center manifold and normal form methods can be used as shown in [10] and [11].

8. VIBRATION SUPPRESSION USING 1:2 IR

In this section we consider establishing modal coupling using 1:2 IR. This type of resonance occurs in the system due to the presence of quadratic nonlinearities. Similar to 1:1 IR, we first consider the problem of tuning the system parameters to establish a 1:2 ratio of the natural frequencies.

8.1 System Parameters

If we set $\Omega_1/\Omega_2 = 2$, using (9) the following equations for s_2 are obtained:

$$s_2 = \frac{(17s_7 + 8s_1s_6) \pm \sqrt{225s_7^2 + 400s_1s_6s_7}}{8} \quad (40)$$

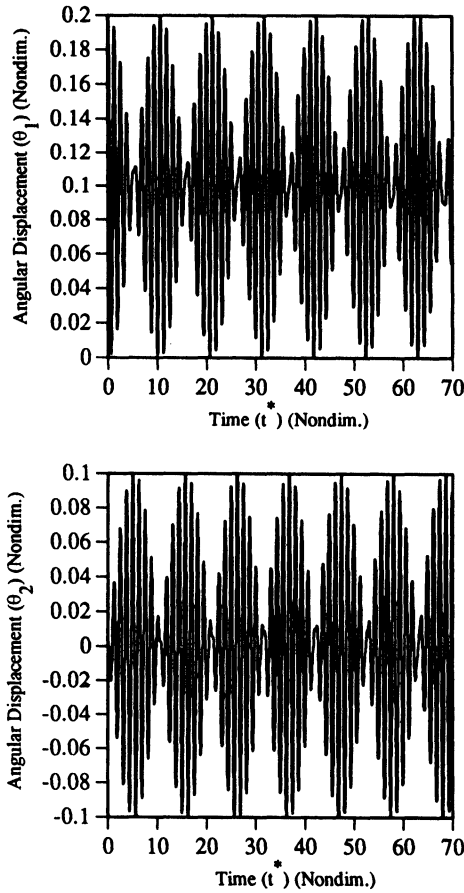


Figure 5 Time response—1:1 IR. $\omega^* = 3.0$, $\omega_{n1}^* = 4.04$, $\omega_{n2}^* = 5.0$, $\theta_{1e} = 0.1$.

Unlike 1:1 IR where the frequencies cannot be tuned to an exact ratio, using (40) it is possible to tune Ω_1 and Ω_2 to an exact 1:2 ratio. In (40), we choose the value of s_2 which gives a real value for ω_{n1}^* . Figure 7 shows a set of tuned parameter values obtained using (40). It can be seen from this figure, that for certain values of ω^* the system can be tuned for 1:2 IR at two different values of ω_{n1}^* , which is not possible in the 1:1 IR case.

8.2 Perturbation Analysis

Although the system can be tuned for an exact 1:2 ratio of Ω_1 and Ω_2 , we still consider a detuning parameter δ because it may not be practically possible to tune the system to an exact ratio. By defining $\delta = \epsilon\sigma$, the frequencies are related through the following equations:

$$\Omega_1 = 2\Omega_2 + \epsilon\sigma \tag{41}$$

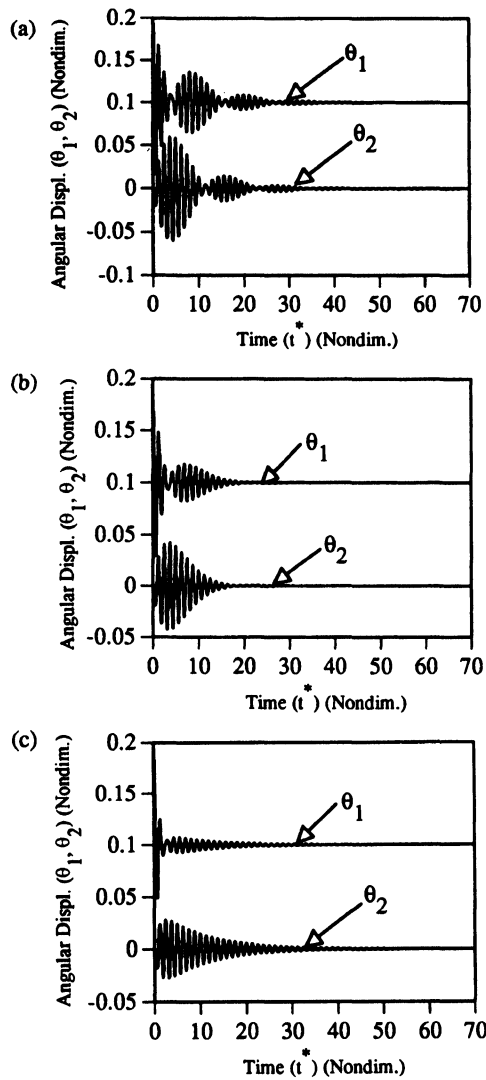


Figure 6 Time response—1:1 IR. $\omega^* = 3.0$, $\omega_{n1}^* = 4.04$, $\omega_{n2}^* = 5.0$, $\theta_{1e} = 0.1$. (a) $C = 0.5$; (b) $C = 1.0$; (c) $C = 2.0$.

Using (41) the following relationships are obtained:

$$\begin{aligned}
 e^{i2\Omega_2 T_0} &= e^{i\Omega_1 T_0} e^{-i\sigma T_1} \\
 e^{i(\Omega_1 - \Omega_2) T_0} &= e^{i\Omega_2 T_0} e^{i\sigma T_1}
 \end{aligned}
 \tag{42}$$

Substituting (42) in *rhs3* and *rhs4* and following a procedure similar to the 1:1 IR case, the following solvability conditions are obtained for 1:2 IR:

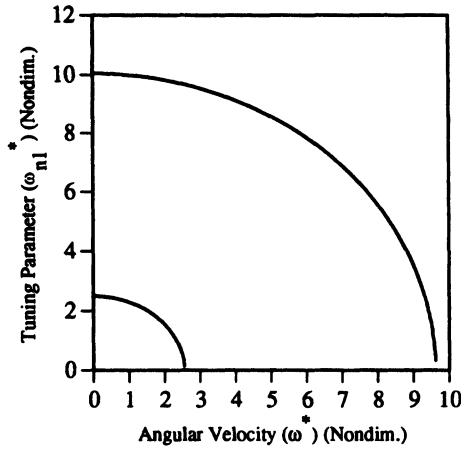


Figure 7 Tuned parameters—1:2 IR. $\omega_{n2}^* = 5.0, \theta_{1e} = 0.1$.

$$\begin{aligned}
 x_{47}A_1' + x_{48}A_2^2e^{-i\sigma T_1} &= 0 \\
 x_{49}A_2' + x_{50}A_1\bar{A}_2e^{i\sigma T_1} &= 0
 \end{aligned}
 \tag{43}$$

where (') indicates differentiation with respect to T_1 , and x_i are constants. Using (35) the complex constants A_1 and A_2 are converted to polar form resulting in the following simplification:

$$\begin{aligned}
 a_1' &= \Gamma_1 a_2^2 \sin(\gamma) \\
 a_2' &= -\Gamma_2 a_1 a_2 \sin(\gamma) \\
 a_1 \alpha_1' &= \Gamma_1 a_2^2 \cos(\gamma) \\
 a_2 \alpha_2' &= \Gamma_2 a_1 \cos(\gamma)
 \end{aligned}
 \tag{44}$$

where

$$\gamma = \sigma T_1 + \alpha_1 - 2\alpha_2
 \tag{45}$$

Combining the last two equations in (44) gives:

$$a_1 \gamma' = \Gamma_1 a_2^2 \cos(\gamma) - 2\Gamma_2 a_1^2 \cos(\gamma) + a_1 \sigma
 \tag{46}$$

and combining the first two equations in (44) gives the following conservation of energy relationship for the modal amplitudes:

$$a_1^2 + \nu a_2^2 = E
 \tag{47}$$

Note that to show modal coupling for 1:2 IR we had to use terms only up to ϵ^2 order. This is typical for 1:2 IR because only quadratic terms contribute to the modal coupling. Figure 8 shows the modal amplitude response on the slow time scale T_1 obtained using (44). The response shows that the amplitudes are coupled but the coupling is not as strong as in 1:1 IR case.

8.3 Numerical Simulations

Figure 9 shows the time response for a set of 1:2 IR tuned parameters. Note that the beat is present but it is not as strong as in 1:1 IR case. Figure 10 shows the damped response for the same set of parameters. Adding damping to the system shows that small oscillations remain in the system which decay very slowly. Although using 1:2 IR the vibrations cannot be suppressed as quickly as 1:1 IR, nevertheless it is still a useful technique when only quadratic couplings are present.

9. VIBRATION SUPPRESSION USING $r_1 = r_2$

In this section we present a new technique for vibration suppression. This method involves tuning the system parameters to make the linear mode shapes equal. These mode shapes are represented by the modal amplitude ratios r_1 and r_2 given by (20). When the mode shapes are made equal the response for θ_1 and θ_2 becomes similar, and upon introducing damping in one direction the oscillations in the other direction are also suppressed. To make the mode shapes equal it requires setting $r_1 = r_2$, which gives the following equation:

$$s_2 = s_7$$

$$\omega_{n1}^{*2} + \omega^{*2} \cos(2\theta_{1e}) + \sin(\theta_{1e}) - \omega_{n2}^{*2} \sec^2(\theta_{1e}) = 0 \tag{48}$$

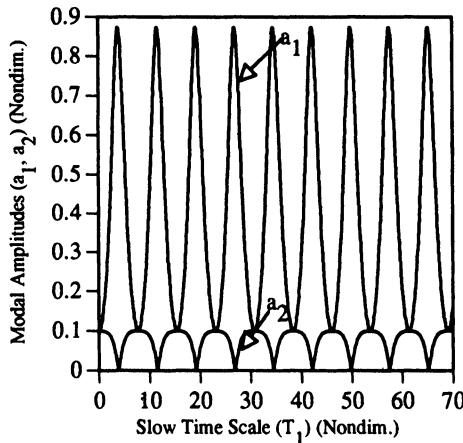


Figure 8 Modal amplitude response—1:2 IR. $\omega^* = 2.0$, $\omega_{n1}^* = 1.54915$, $\omega_{n2}^* = 5.0$, $\theta_{1e} = 0.1$, $\sigma = 0.0$.

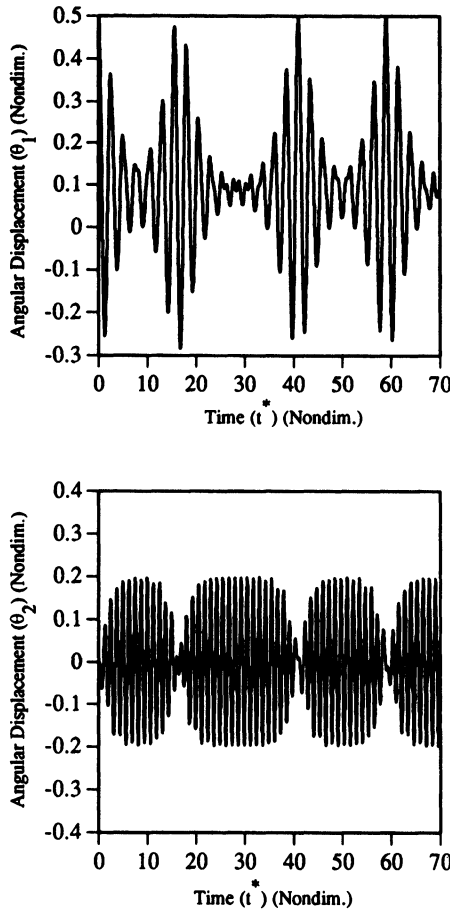


Figure 9 Time response—1:2 IR. $\omega^* = 2.0$, $\omega_{n1}^* = 1.54915$, $\omega_{n2}^* = 5.0$, $\theta_{1e} = 0.1$.

Note that the above equations are the same as (23) which were obtained by minimizing the difference between the frequencies with respect to ω_{n1}^* . This implies that the difference between the frequencies (δ) can be obtained from (24), and for small values of θ_{1e} the difference is small and both $r_1 = r_2$ and 1:1 IR give the same results. When θ_{1e} is not small the difference between the frequencies Ω_1 and Ω_2 is large and the system does not exhibit 1:1 IR, however the mode shapes are identical (*i.e.*, $r_1 = r_2$). Figure 11 shows the numerical simulation results for this case for damped and undamped conditions. The response is nonresonant but still gives very good vibration suppression results. Some applications may not allow tuning the equilibrium positions to large values; in such cases we have to rely on tuning ω_{n1}^* to establish $r_1 = r_2$ for which the range is limited. To overcome this problem, we present a method to obtain a control torque which will make the system satisfy $r_1 = r_2$, regardless of the values of the system parameters.

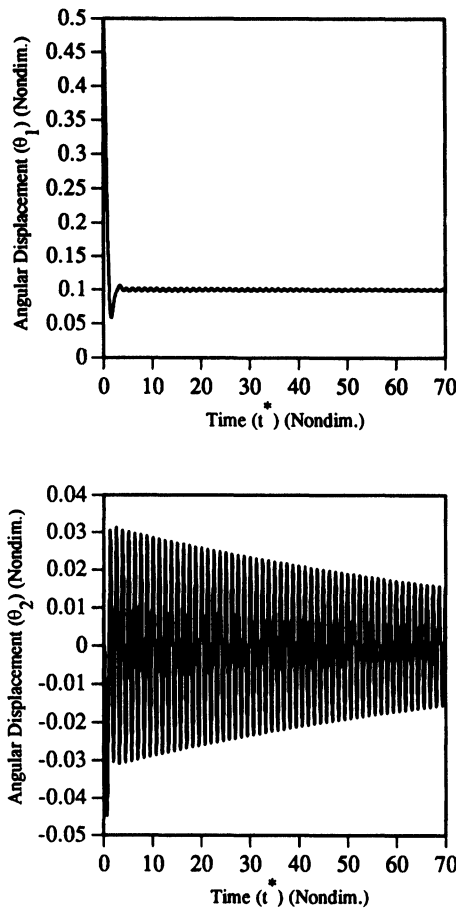


Figure 10 Time response—1:2 IR. $\omega^* = 2.0$, $\omega_{n1}^* = 1.54915$, $\omega_{n2}^* = 5.0$, $\theta_{1e} = 0.1$, $C = 3.0$.

9.1 Control Torque for $r_1 = r_2$

To make the system exhibit $r_1 = r_2$, the condition $s_2 = s_7$ has to be satisfied. To achieve this we modify the control torque T^* so that in the linearized equations of motion (8) the s_2 term becomes equal to s_7 . It can be seen that if choose T^* as:

$$\begin{aligned} T^* &= -(s_2 - s_7)\theta_1 + T_c + C\dot{\theta}_1^* \\ &= -(\omega_{n1}^{*2} + \omega^{*2} \cos(2\theta_{1e}) + \sin(\theta_{1e}) - \omega_{n2}^{*2} \sec^2(\theta_{1e}))\theta_1 + T_c + C\dot{\theta}_1^* \end{aligned} \quad (49)$$

after the differentiation involved in the linearization using Taylor series, in (8), s_2 becomes equal to s_7 . In (49), the term T_c is a constant, which is used to establish the equilibrium position. With the modification of T^* as in (49), the equations for the equilibrium positions

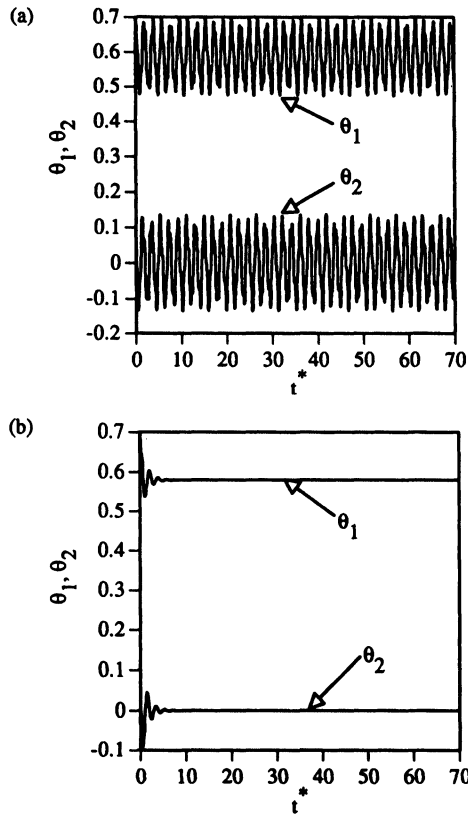


Figure 11 Time response— $r_1 = r_2$, $\omega^* = 7.0$, $\omega_{n1}^* = 4.0$, $\omega_{n2}^* = 5.0$, $\theta_{1e} = 0.58$. (a) $C = 0.0$; (b) $C = 6.0$.

(7) become:

$$\begin{aligned}
 \omega_{n1}^{*2} \theta_{1e} + \frac{1}{2} \omega^{*2} \sin(\theta_{1e}) - \cos(\theta_{1e}) - (\omega_{n1}^{*2} + \omega^{*2} \cos(2\theta_{1e})) \\
 + \sin(\theta_{1e}) - \omega_{n2}^{*2} \sec^2(\theta_{1e}) \theta_{1e} + T_c^* = 0 \\
 \omega_{n2}^{*2} \theta_{2e} = 0 \tag{50}
 \end{aligned}$$

Given a set of parameters, the value of T_c^* required to achieve a desired equilibrium position is obtained from (50).

With the generalizations introduced in this section we can see the effect of establishing the modal coupling for a given set of parameters. Figure 12(a) shows the response of the system when the control torque is not applied (only damping is introduced using velocity feedback), and Figure 12 (b) shows the effect of applying the control torque to establish $r_1 = r_2$. It can be clearly seen that when modal coupling is established the vibrations are quickly suppressed.

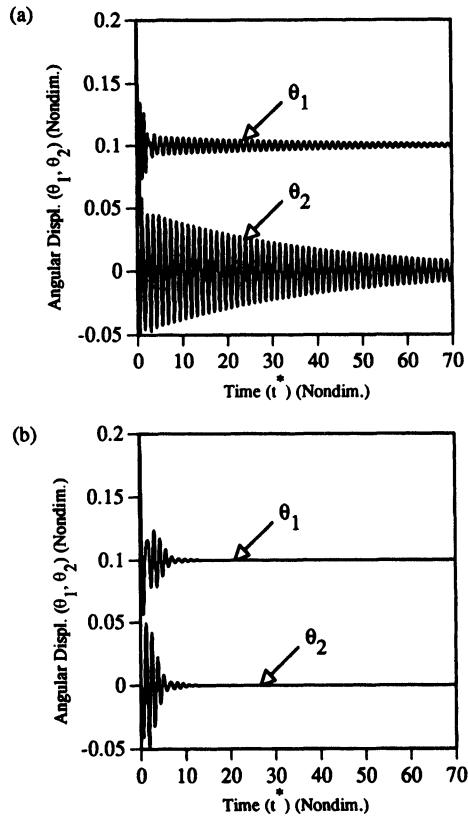


Figure 12 Time response— $r_1 = r_2$, $\omega^* = 7.0$, $\omega_{n1}^* = 4.0$, $\omega_{n2}^* = 5.0$, $\theta_{1e} = 0.58$, $C = 2.0$. (a) $r_1 \neq r_2$; (b) $r_1 = r_2$.

10. CONCLUSION

In this paper we have discussed vibration suppression of a two-degree-of-freedom flexible gyroscopic system using modal coupling. When modal coupling is established a strong energy link is formed between the modes which is used to transfer energy from the uncontrolled mode to the controlled mode from where it is dissipated. The equations of motion show that the system is coupled through linear, quadratic, and cubic terms, indicating that the coupling can be enhanced using 1:1 and 1:2 IR ratios. A study of the system parameters reveal that the system cannot be tuned to establish an exact 1:1 IR ratio. However, it was shown that for small values of the equilibrium position θ_{1e} , the frequencies can be approximated as 1:1 IR. It was also shown the range of the tuning parameter to establish a desired IR ratio was limited. To overcome this a control torque was introduced which upon application makes the system exhibit modal coupling, regardless of the choice of the system parameters.

The modal interaction under Internal Resonance conditions was ascertained analytically using the perturbation method of multiple scales. Results indicate that when 1:1 IR was

established the modal interactions were strong and the vibrations were suppressed quickly. However for 1:2 IR the modal coupling was not as strong as in 1:1 IR case resulting in oscillations which continued to exist for a long period of time. A new method was presented based on the equality of the mode shapes ($r_1 = r_2$), which is a generalization of 1:1 IR. Using this method a strong modal interaction was established even under nonresonant conditions.

References

1. M.F. Golnaraghi, Vibration Suppression of Flexible Structures Using Internal Resonance, *Mechanics Research Communications Journal* **18-2/3** (1991), 135–143.
2. M.F. Golnaraghi, Regulation of Flexible Structures via Nonlinear Coupling, *Journal of Dynamics and Controls* **1** (1991), 405–428.
3. K.L. Tuer, A.P. Duquette, and M.F. Golnaraghi, Vibration Control of a Flexible Beam Using a Rotational Internal Resonance Controller, Part 1: Theoretical Development and Analysis, *Journal of Sound and Vibrations* **167-1** (1993), 41–62.
4. A.P. Duquette, K.L. Tuer, and M.F. Golnaraghi, Vibration Control of a Flexible Beam Using a Rotational Internal Resonance Controller, Part 2: Experiment, *Journal of Sound and Vibrations* **167-1** (1993), 63–75.
5. K.L. Tuer, Vibration Control of Flexible Structures Using Nonlinear and Linear Coupling Effects, *M.A.Sc. Thesis*, Department of Mechanical Engineering, University of Waterloo Ontario, Canada, 1991.
6. A.P. Duquette, An Experimental Study of Vibration Control of a Flexible Beam Via Modal and Coordinate Coupling, *M.A.Sc. Thesis*, Department of Mechanical Engineering, University of Waterloo Ontario, Canada, 1991.
7. K.L. Tuer, M.F. Golnaraghi, and D. Wang, Development of a Generalized Active Vibration Suppression Strategy for a Cantilever Beam Using Internal Resonance *Journal of Nonlinear Dynamics* **5** (1994), 131–151.
8. K.L. Tuer, M.F. Golnaraghi, and D. Wang, Towards a Generalized Regulation Scheme for Oscillatory Systems via Coupling Effects, *IEEE Trans. On Automatic Control* **60(3)** (1995), 522–530.
9. S. Oueini, and M.F. Golnaraghi, Experimental Implementation of the Internal Resonance Control Strategy, Accepted for Publication, *Journal of Sound and Vibration* (1995).
10. A. Khajepour, M.F. Golnaraghi, and K.A. Morris, Internal Resonance Controller Design Using Normal Forms, *Proc., International Mechanical Engineering Congress and Exposition*, AMD-Vol. 192/DE-Vol. 78, 143–150, 1994.
11. A. Khajepour, M.F. Golnaraghi, and K.A. Morris, Vibration Suppression of a Flexible Beam Using Center Manifold Theory, To appear in *Proc., 15th. ASME Biennial Conference in Mechanical Engineering, Vibrations and Noise*, Sept. 17–21, 1995.
12. P.R. Sethna, Vibrations of Dynamical Systems with Quadratic Nonlinearities, *Journal of Applied Mechanics* **32** (1965), 576–582.
13. W. Stupnicka, On the Phenomenon of the Combination Type Resonance in Nonlinear Two-Degree of Freedom Systems, *International Journal of Non-Linear Mechanics* **4** (1969), 335–359.
14. R. Van Dooren, Combination Tones of Summed Type in a Nonlinear Damped Vibratory System with Two-Degrees of Freedom, *International Journal of Non-Linear Mechanics* **6** (1969), 237–254.
15. A.G. Haddow, and D.T. Mook, Theoretical and Experimental Study of Modal Interaction in a Two-Degree of Freedom Structure, *Journal of Sound and Vibration* **97** (1984), 451–473.
16. D.T. Mook, R.H. Plaut, and N. HaQuang, The Influence of Internal Resonance on Nonlinear Structural Vibrations under Subharmonic Resonance Conditions, *Journal of Sound and Vibration* **102-4** (1985), 473–492.
17. A.H. Nayfeh, and D.T. Mook, *Nonlinear Oscillations*, John Wiley & Sons New York, 1979.
18. A.R.S. Bramwell, *Helicopter Dynamics*, Edward Arnold Ltd. London, 1976.
19. R.L. Bielawa, *Rotary Wing Structural Dynamics and Aeroelasticity*, AIAA Education series Washington DC, 1992.
20. S.A.Q. Siddiqui, Vibration Suppression and Stability in Gyroscopic Systems, *M.A.Sc. Thesis*, Department of Mechanical Engineering, University of Waterloo Ontario, Canada, 1994.
21. A.H. Nayfeh, *Introduction to Perturbation Techniques*, John Wiley & Sons, New York, 1981.

Special Issue on Space Dynamics

Call for Papers

Space dynamics is a very general title that can accommodate a long list of activities. This kind of research started with the study of the motion of the stars and the planets back to the origin of astronomy, and nowadays it has a large list of topics. It is possible to make a division in two main categories: astronomy and astrodynamics. By astronomy, we can relate topics that deal with the motion of the planets, natural satellites, comets, and so forth. Many important topics of research nowadays are related to those subjects. By astrodynamics, we mean topics related to spaceflight dynamics.

It means topics where a satellite, a rocket, or any kind of man-made object is travelling in space governed by the gravitational forces of celestial bodies and/or forces generated by propulsion systems that are available in those objects. Many topics are related to orbit determination, propagation, and orbital maneuvers related to those spacecrafts. Several other topics that are related to this subject are numerical methods, nonlinear dynamics, chaos, and control.

The main objective of this Special Issue is to publish topics that are under study in one of those lines. The idea is to get the most recent researches and published them in a very short time, so we can give a step in order to help scientists and engineers that work in this field to be aware of actual research. All the published papers have to be peer reviewed, but in a fast and accurate way so that the topics are not outdated by the large speed that the information flows nowadays.

Before submission authors should carefully read over the journal's Author Guidelines, which are located at <http://www.hindawi.com/journals/mpe/guidelines.html>. Prospective authors should submit an electronic copy of their complete manuscript through the journal Manuscript Tracking System at <http://mts.hindawi.com/> according to the following timetable:

Manuscript Due	July 1, 2009
First Round of Reviews	October 1, 2009
Publication Date	January 1, 2010

Lead Guest Editor

Antonio F. Bertachini A. Prado, Instituto Nacional de Pesquisas Espaciais (INPE), São José dos Campos, 12227-010 São Paulo, Brazil; prado@dem.inpe.br

Guest Editors

Maria Cecilia Zanardi, São Paulo State University (UNESP), Guaratinguetá, 12516-410 São Paulo, Brazil; cecilia@feg.unesp.br

Tadashi Yokoyama, Universidade Estadual Paulista (UNESP), Rio Claro, 13506-900 São Paulo, Brazil; tadashi@rc.unesp.br

Silvia Maria Giuliatti Winter, São Paulo State University (UNESP), Guaratinguetá, 12516-410 São Paulo, Brazil; silvia@feg.unesp.br